Journal of Magnetism and Magnetic Materials 592 (2024) 171796

Contents lists available at ScienceDirect

Journal of Magnetism and Magnetic Materials

journal homepage: www.elsevier.com/locate/jmmm

Application of active thermography for the study of losses in components produced by laser powder Bed fusion

Michele Quercio [a,*], Emir Poskovic [b], Fausto Franchini [b], Elisa Fracchia [c], Luca Ferraris [b], Aldo Canova [b], Alberto Tenconi [b], Hans Tiismus [d], Ants Kallaste [d]

[a] Department of Industrial, Electronic and Mechanical Engineering, Università degli studi Roma Tre, Via Vito Volterra 62 - Ex Vasca Navale, Roma 00146, Italy
[b] Energy Department, Politecnico di Torino, Corso Duca Degli Abruzzi 24, Torino 10129, Italy
[c] Department of Management and Production Engineering (DIGEP), Politecnico di Torino, Viale Teresa Michel 5, Alessandria, Italy
[d] Tallin University of Technology, Department of Electrical Power Engineering and Mechatronic, 5, Ehitajate tee, Tallin 19086, Estonia

ARTICLE INFO

Keywords:
Additive Manufacturing
Ferromagnetic material
Non destructive testing
Thermography

ABSTRACT

The quality of the components produced is guaranteed by two types of methods, destructive and non-destructive (NDT). In the first case, a product that corresponds to a specific production lot is taken and it is broken to evaluate its properties. Instead, in the case of non-destructive testing, the piece is not sacrificed but the mechanical, electrical, and magnetic properties of the piece in question are obtained through special techniques. These NDT techniques are very interesting in the case of pieces produced using Additive Manufacturing (AM) technology. The reason lies in the fact that production volumes are low, and the costs of raw materials and electricity are currently high, therefore production waste is reduced. This work focuses on the use of the active thermography technique as a tool for characterizing the electrical and magnetic properties of a component produced using the Laser Powder Bed Fusion (LPBF) technique in FeSi2.9% ferromagnetic material. The results of this investigation are very interesting, as they allowed the authors to characterize the losses of this material both from a qualitative and quantitative point of view. The choice of this material lies in the fact that it is also widely used in the literature as a material for the construction of AM electric motors. This kind of characterization, exploiting the active thermography technique, is a novelty for this kind of material produced using the LPBF technique.

1. Introduction

Additive manufacturing (AM) has revolutionized the manufacturing industry by enabling the production of complex geometries with high precision and accuracy. Also, the considerable versatility in several industrial sectors permits new solutions with respect to traditional techniques [1–3]. A specific field of applications consists of electrical devices such as electrical machines, sensors, inductors, etc., where ferromagnetic or conducting materials produced by AM could resolve some drawbacks [4–8]. AM ferromagnetic materials show high potential to replace traditional ones [9–13]. For instance, in the case of soft magnetic materials, the AM soft magnets allow more geometric design with respect to laminated steels and more magnetic properties compared to Soft Magnetic Composites (SMC [14]) [15–19]. In the case of AM permanent magnets [20], the comparison can be made with the bonded magnets [21–27]. The processes and solutions are various, and different criticisms could affect the final product.

The process of AM generally involves the layer-by-layer deposition of materials to create a three-dimensional (3D) object. This process offers several advantages over conventional manufacturing methods, including reduced waste and increased design flexibility. However, the AM process can lead to the formation of defects and discontinuities that can compromise the performance and quality of the final product. One of the critical issues in AM ferromagnetic materials is the occurrence of unforeseen iron losses, which can result in reduced efficiency and increased costs. The origin of these losses can occur due to various factors, such as material shrinkage, warping, porosity, and incomplete fusion between layers. These losses can significantly impact the final product's mechanical and electromagnetic properties and functional performance, particularly in applications with high strength and efficiency. Therefore, there is a need for effective methods to study and quantify losses due to process steps in the AM components.

* Correspondig author.
E-mail addresses: michele.quercio@uniroma3.it (M. Quercio), hans.tiismus@taltech.ee (H. Tiismus), ants.kallaste@taltech.ee (A. Kallaste).

https://doi.org/10.1016/j.jmmm.2024.171796
Received 30 November 2023; Received in revised form 25 January 2024; Accepted 25 January 2024
Available online 30 January 2024

Table 1
Process parameters used to manufacture the ferromagnetic shields.

Process parameters	Value
Laser power, P (W)	250 (primary)/ 100 (secondary)
Scan speed, v (m/s)	0.5
Hatch distance, h_d (μm)	120
Layer thickness, z (μm)	50
Laser spot size (μm)	120
Preheating	NA
Environment	Nitrogen
Oxygen content	0.1 %
Scan strategy	Stripes

Non-destructive testing (NDT) techniques are widely proposed in manufacturing to detect and characterize material defects without damaging the component [28]. NDT techniques could provide valuable information about the quality and integrity of AM components [29–32], allowing manufacturers to identify and address issues before they become critical. This scientific article focuses on the active thermography approach, a non-destructive testing technique that uses heat to detect and characterize defects in materials [33]. Active thermography involves the application of a heat source to the surface of the material and the measurement of the resulting thermal response. The heat source can be applied using various methods, such as flash lamps, lasers, or induction heating [34,35]. The thermal response is then measured using an infrared camera or other thermal imaging device. The principles of active thermography are based on the fact that defects in materials have different thermal properties than the surrounding material. For example, a void or crack in a material will have a different thermal conductivity and heat capacity than the surrounding material. When a heat source is applied to the surface of the material, the thermal response of the material will be affected by the presence of defects. By analyzing the thermal response, it is possible to detect and characterize defects in the material. Active thermography has several advantages over other NDT techniques. It is a non-contact method, which means that it does not require direct contact with the material being tested [33]. This makes it suitable for testing delicate or fragile materials that other NDT techniques could damage.

Active thermography is also a robust and efficient method, allowing large areas to be scanned to minimum detail. It is also a relatively inexpensive technique, requiring only a heat source and an infrared camera. However, active thermography also has some limitations. It is sensitive to surface conditions, such as surface roughness or contamination, which can affect the accuracy of the results [33]. The technique is also limited to detecting defects close to the material's surface [34]. More profound defects cannot be detected using this method. Despite these limitations, active thermography has shown great potential for the study of defects and drawbacks in AM components. The technique has been used to detect and characterize various defects in AM components, including porosity, incomplete fusion, and delamination. By identifying these defects early in the manufacturing process, manufacturers can take corrective action to improve the quality and reliability of their products.

This article discusses the principles and applications of active thermography for the study of the distribution of iron losses in AM components. The advantages and limitations of this technique and a case study are presented to demonstrate its effectiveness in improving the quality and reliability of AM products.

2. Materials and methods

The material examined is FeSi2.9 % [36], the ferromagnetic material used to produce components for electrical devices, for example, rotors of electric motors. This alloy with this low percentage of silicon was chosen because it is the most used in conventional production methods [37]. In some works, components have been produced with a much higher percentage of silicon [38,39], which, to the detriment of the mechanical properties, allows for better performance from a magnetic point of view. Samples were prepared using an SLM Solutions GmbH Realizer SLM-280 machine, which has a large build envelope and dual-scanning yttrium lasers. For research purposes, a custom, smaller build platform and recoater were created to reduce raw powder quantity and streamline powder exchange between projects. The samples were printed using a laser remelting strategy, with printing parameters suitable for achieving approximately 99 % relative density in Fe-Si parts as reported in Table 1. The printing was done in a nitrogen inert gas environment, and preheating was not used due to the limitations of the custom build platform. Sandvik group provided pre-alloyed Fe-Si powder, which was used to create specimens through selective laser melting (SLM). The powder's chemical composition was analyzed using energy-dispersive X-ray spectroscopy (EDX) and atomic emission spectroscopy (AES). The powder comprised approximately spherical particles ranging in size from 29 to 58 μm, with a median diameter of 38 μm (d50). The size distribution of the powder was determined using a laser-scattering particle size distribution analyzer in a water-dispersive environment, and the particle shape was confirmed using scanning electron microscopy (SEM). Since the application of this material is purely in the electromagnetic field, we evaluated the energetic and magnetic performance; the single sheet tester (SST) is used to assess permeability, hysteresis loop and iron losses. These investigations were conducted on ad hoc samples and reported in Table II with the list of their functions and a close-up view of the artefact. The measurements were carried out on the sample after heat treatment at 1200 °C in a vacuum for 1 h. The magnetic characterization is performed with a self-built and self-programmed soft materials hysteresigraph, controlled by a LabVIEW Virtual Instrument (2012 edition) on a PC. The hysteresigraph software guests a driver to low-level communication with an IR camera (Optris

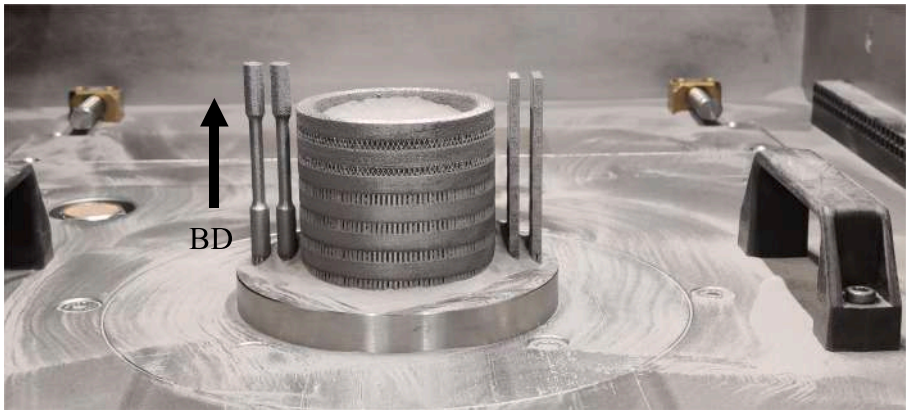

Fig. 1. Illustration of production direction.

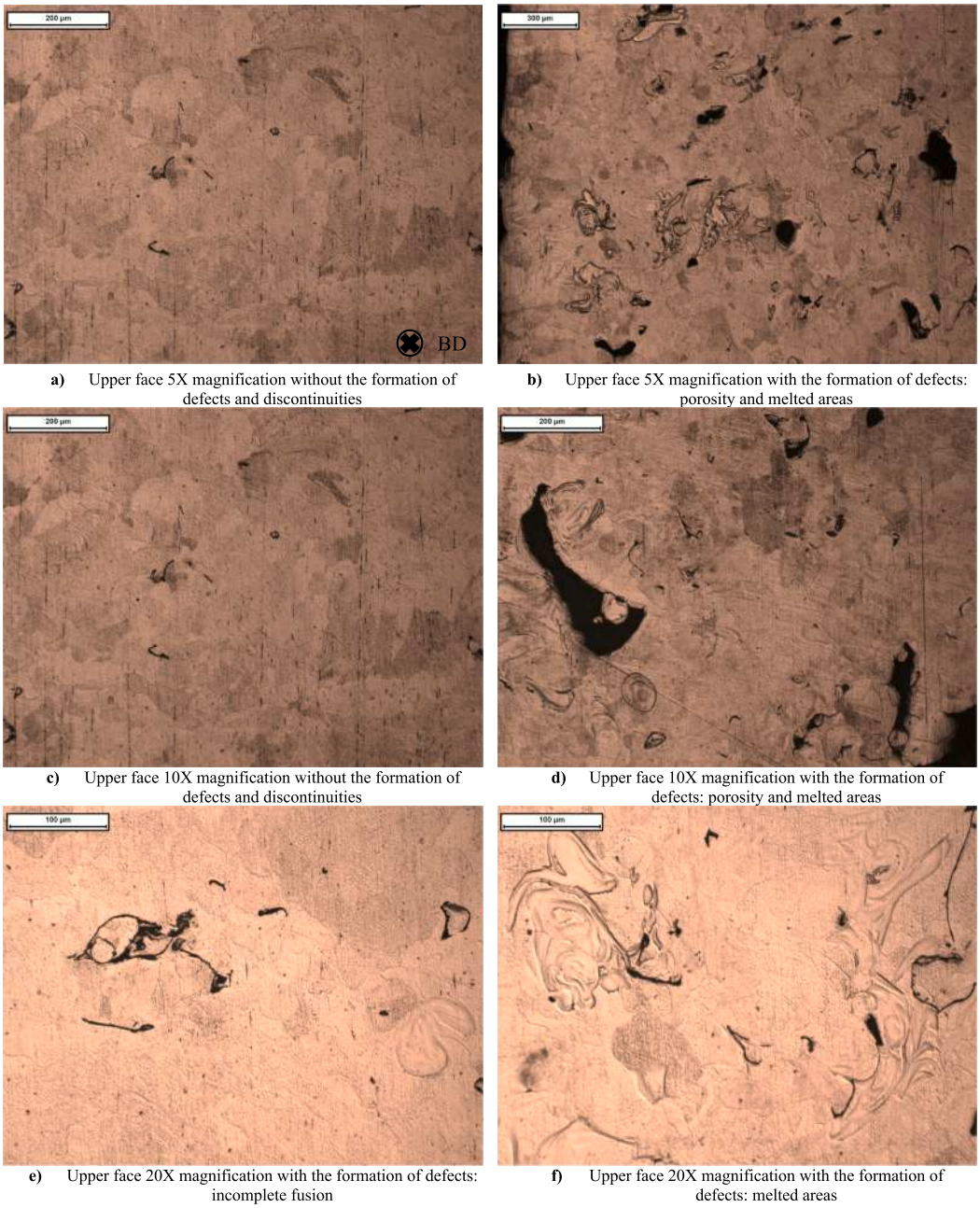

a) Upper face 5X magnification without the formation of defects and discontinuities

b) Upper face 5X magnification with the formation of defects: porosity and melted areas

c) Upper face 10X magnification without the formation of defects and discontinuities

d) Upper face 10X magnification with the formation of defects: porosity and melted areas

e) Upper face 20X magnification with the formation of defects: incomplete fusion

f) Upper face 20X magnification with the formation of defects: melted areas

Fig. 2. Microstructural analysis by means of the optical microscope on the upper face (growth build face) after heat treatment at 1200 °C; the output direction BD is only reported in a) but is valid for all images.

Model OPTPI45ILTO29T090). The results of these experiments are reported in the dedicated chapter.

3. Microstructural analysis

Before starting with metallographic characterization, it is necessary to explain some operation conditions. The build direction (BD) of the specimens is illustrated in Fig. 1 along the vertical axis. The tiny tile used for microstructural analysis was obtained from this production step. The final products generally show good aspects. On the other hand, some zones could hide the defects, and the thermographic method is implemented to discover possible imperfections. The microstructural analysis is conducted to determine the defects' origin [40,41] and possibly connect with iron losses by observing two surfaces: the upper face and the face parallel to the build.

The microstructural properties after heat treatment were evaluated. The graphs in Fig. 2 show the characteristics of the upper; some areas have different formations of defects, especially porosity and particular melted zones. Instead, in Fig. 3, the face parallel to the build direction shows that the microstructure is columnar with elongated grains along the printing direction (BD) [42,43]. On this surface, it is possible to note the potential melt pools and incomplete fusion, as shown in Fig. 3f. The microscopic presence of the defects itself does not immediately mean the location of losses, but low magnetic properties and the necessity for optimising the printing process. The effect of the heat treatment modifies the microstructure, characterizing it by larger, coarser, and wider grains together with small columnar grains [44]. The grains' growth reduces the grains' boundaries, which has been seen to influence the magnetic properties as the latter hinders the orientation of the magnetic domains.

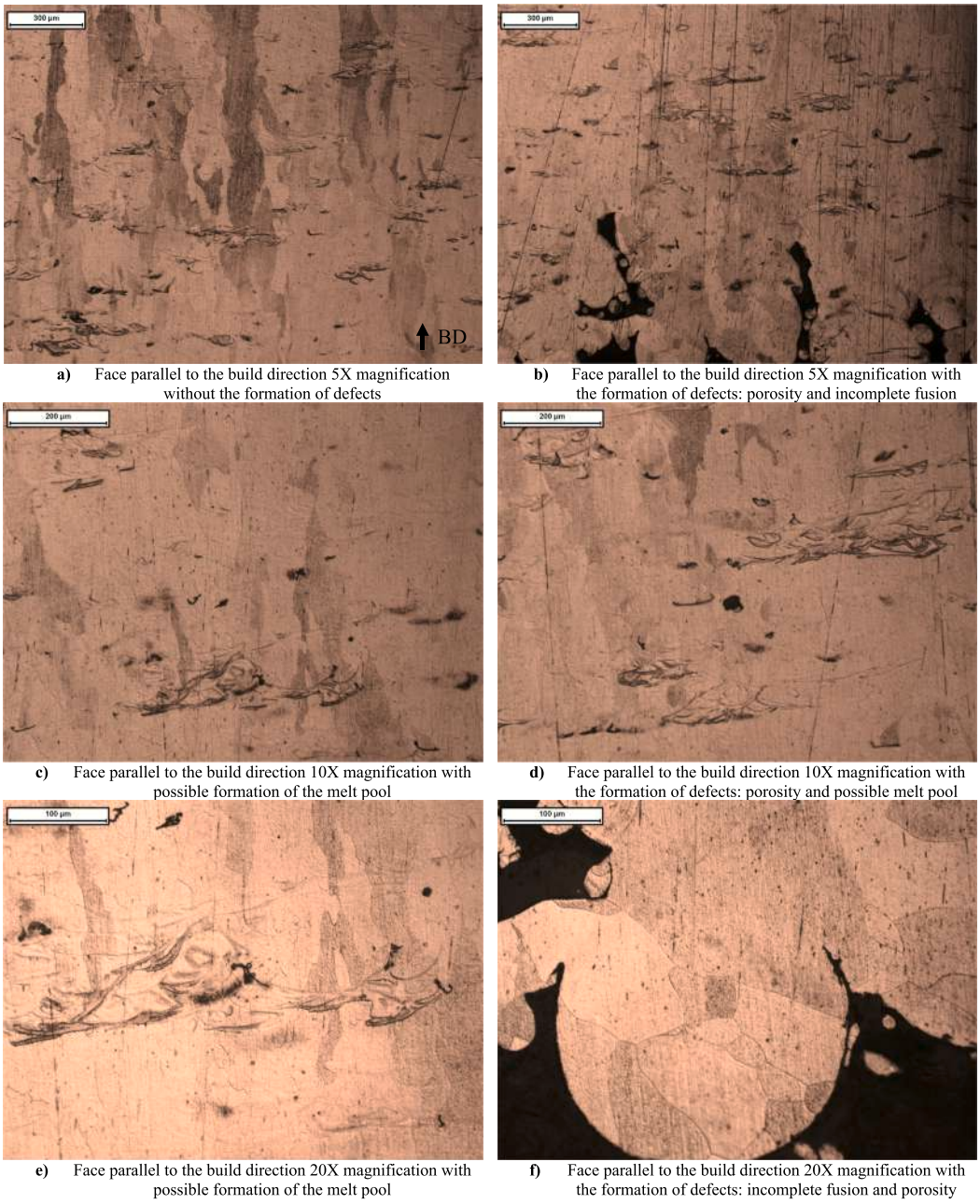

a) Face parallel to the build direction 5X magnification without the formation of defects

b) Face parallel to the build direction 5X magnification with the formation of defects: porosity and incomplete fusion

c) Face parallel to the build direction 10X magnification with possible formation of the melt pool

d) Face parallel to the build direction 10X magnification with the formation of defects: porosity and possible melt pool

e) Face parallel to the build direction 20X magnification with possible formation of the melt pool

f) Face parallel to the build direction 20X magnification with the formation of defects: incomplete fusion and porosity

Fig. 3. Microstructural analysis by means of the optical microscope on the face parallel to the build direction after heat treatment at 1200 °C; the direction BD is only reported in a) but is valid for all images.

4. Magnetic measurements

4.1. Single sheet tester

The characterization based on the single sheet tester (SST) method is performed on laminated steel and SMC materials [45–49]. The same technique is used to measure the magnetic and energetic of additive manufacturing thin parallelepiped sample (produced bar of about 7 x 10 x 42 mm). The method does not require to be wound, making it possible, in this way, to immediately perform the measurements, saving and optimizing the time of the specimen preparation process. The single sheet tester is equipped with a secondary winding placed around the middle of the sample and a split primary winding at both sides, as shown in Fig. 4 [45].

The SST method has a faster application compared to other magnetic tests, and eventual doubts related to the reliability of the results should require calibration using another standard test, which, in the case of additive manufacturing materials, is the toroid test.

For the measurements to be correct, a sinusoidal power supply waveform must be guaranteed; therefore, the harmonic contribution must be low. For this reason, the equipment used can ensure a total harmonic distortion of the flux less than 1 %. The measurements were conducted in a frequency range between 10 Hz and 1 kHz, limited to a voltage peak on the secondary equal to 10 V. The results were acquired using the LabVIEW software and a National Instruments data acquisition card and are shown from Figs. 5–8. The data show clear differences between the BH curves, magnetic permeability, hysteresis loop, and total iron losses trends along the frequency ranges. As can be seen, the maximum μr is 3200 and magnetic induction reaches about 1.2 T. The low magnetic induction value can be associated with the formation of defects such as porosity and melted areas. The total iron losses, represented by the area formed by the hysteresis cycle, show the presence of

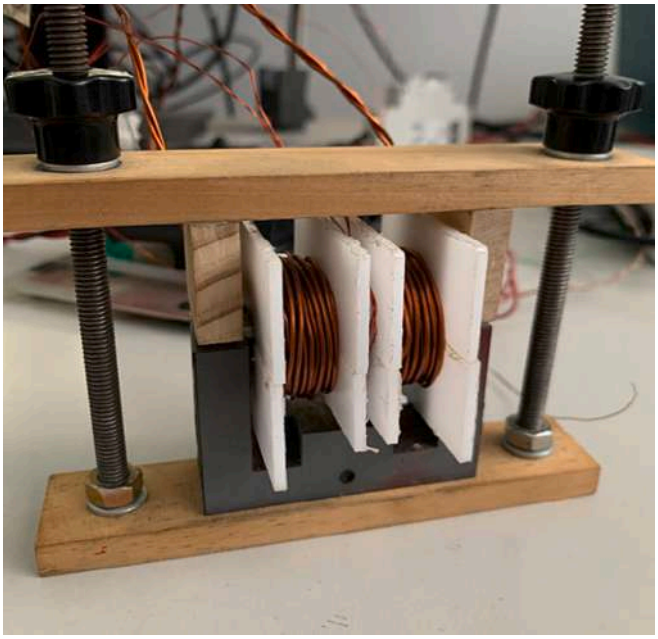

Fig. 4. Single sheet tester setup used for the magnetic measurements.

eddy current losses at high-frequency values, as reported in Fig. 8. Furthermore, the reduction of the Hc value for low frequencies involves hysteresis losses is also reduced.

5. Active thermography approach

The active thermography is a conceptually simple method. It involves the sample heating and two thermographic recordings before and after the heating phase. The overtemperature image, emerging from the difference between the two recordings, usually has very low information content, being the overtemperatures in the order of a few mK. In most cases, an adequate signal-to-noise ratio can be obtained only with the iteration of a large number of heating and cooling phases and with the average temperature image over the whole repetition recording set.

The commercially available IR sensors and cameras show a consistent noise contribution and a relatively poor thermal resolution. Thanks to the average operation and the intrinsic noise content, the actual final resolution and sensitivity improve almost linearly up to thousands of repetitions.

In the present work, the thermography analyses were conducted with the same hysteresigraph used for the magnetic characterization. This apparatus hosts a thermal camera interface, integrating both the magnetic stimulus generation and the thermal image acquisition. Once the magnetic characterization is performed, the software saves the stimulus waveform of a specified magnetic condition (a stated flux density, magnetic field or loss level). The stimulus, together with a cooling phase, is then applied to the sample thousands of times, and the overtemperatures are recorded as described before. The result is a single, averaged thermal image representing the total loss distribution on the visible sample surface. The losses are obtained with the following equation ΔT (°C)*cs (J/°Ckg)/excitation time*weight of the sample. The block scheme of the proposed apparatus and its functions are illustrated in Fig. 9.

5.1. Cube sample

The technique was applied using Helmholtz coils as a thermal source and a cube as a sample, as shown in Fig. 10. The main advantage of such a coil is providing adequate excitation without covering the sample surface with windings. On the contrary, the Helmholtz arrangement can hardly produce high excitation levels since this would require much more power than with concentrated coils. The tests were carried out on two magnetization directions considered the build direction, particularly the one along the printing direction and the perpendicular one.

The iron losses distribution in the case of perpendicular magnetization with respect to growth direction is shown in Fig. 11. The magnetic flux goes through the sample in an easy way; this is confirmed by very low losses, 1 ÷ 2 W, in the middle of the cube. The magnetic flux is probably conducted better on the single layer/plane. The high losses are observed on the extreme faces, upper and lower ones. In those areas, the

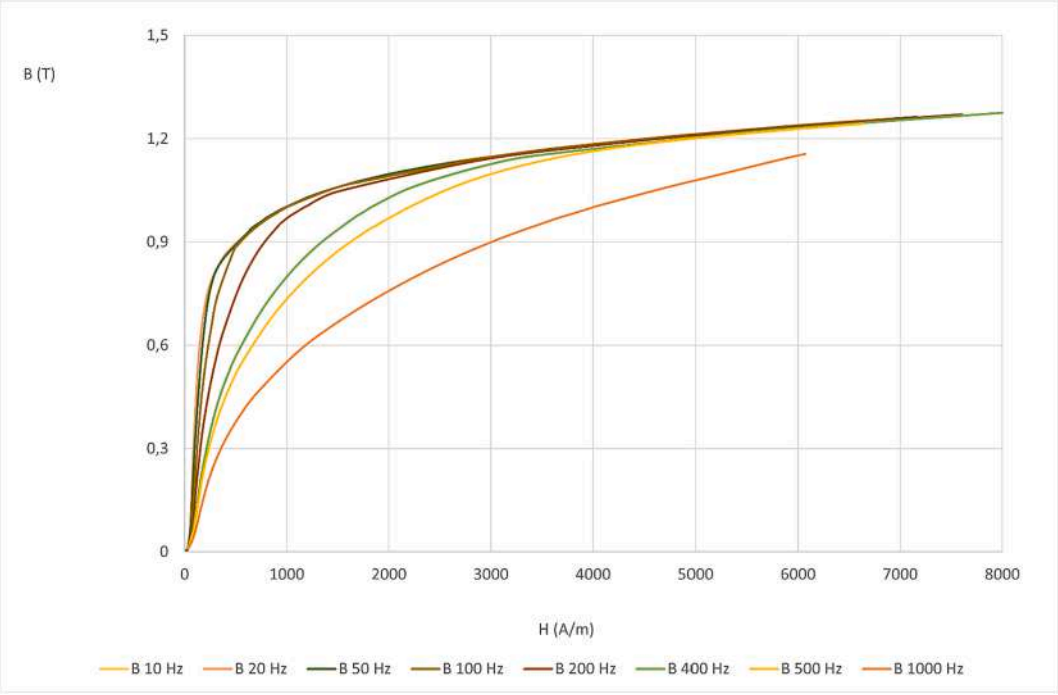

Fig. 5. Magnetization curves at different frequencies after heat treatment at 1200 °C.

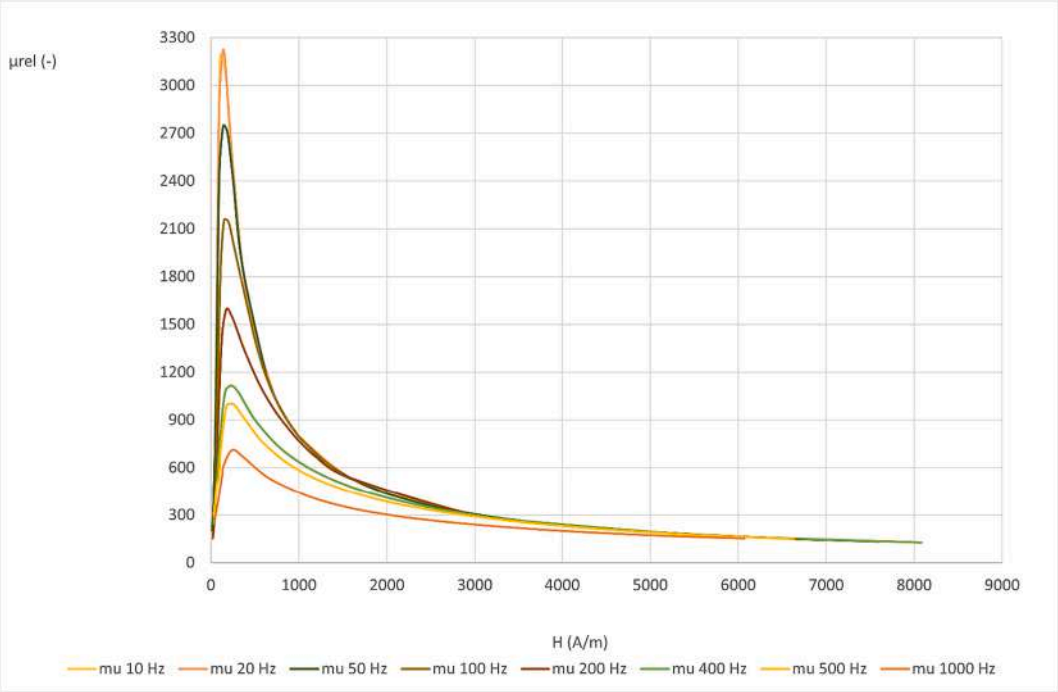

Fig. 6. Magnetic permeability as a function of magnetic field H at different frequencies after heat treatment at 1200 °C.

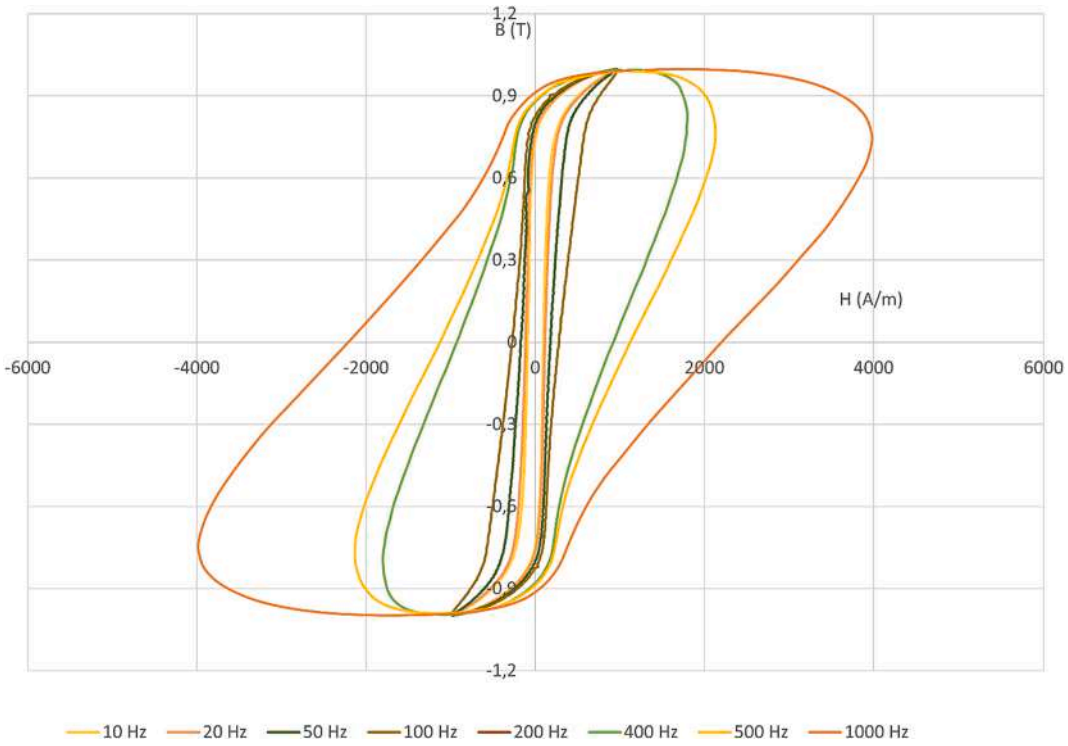

Fig. 7. Hysteresis cycles at different frequencies after heat treatment at 1200 °C.

eddy current losses values are between 7.5 ÷ 9 W. These losses are probably due to mechanical separation from the baseline plate (lower face) and the unwanted melted phenomena (upper face).

Fig. 12 shows the iron losses distribution in the case with magnetization along the growth direction. The iron losses show a more homogeneous distribution and a value between 3.5 and 4 W. On the other hand, the total iron losses on the cube are higher overall than in the case of magnetization perpendicular to the build direction. The reason lies in the magnetic flux, which is conducted with difficulty between layers/planes and also, the eddy currents are limited to every layer. That means total iron losses are affected by the number of deposited layers if the magnetic flux is applied in the build direction.

5.2. *Bar sample*

In the case of the bar sample, the magnetization is obtained with the

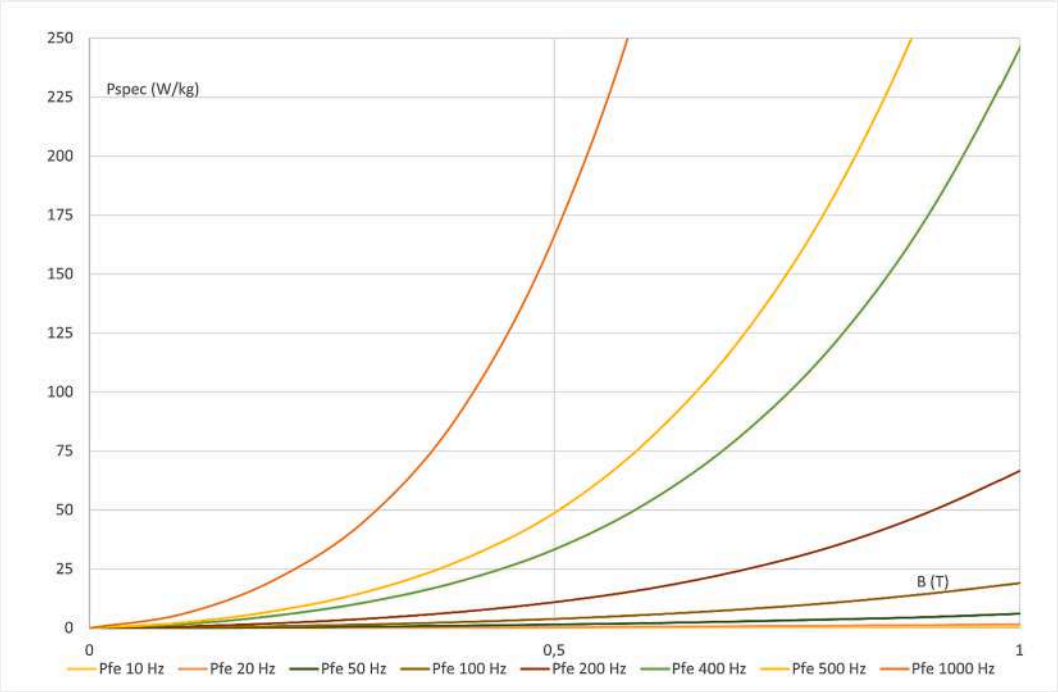

Fig. 8. Specific iron losses as a function of magnetic induction at different frequencies restricted to 250 W/kg after heat treatment at 1200 °C.

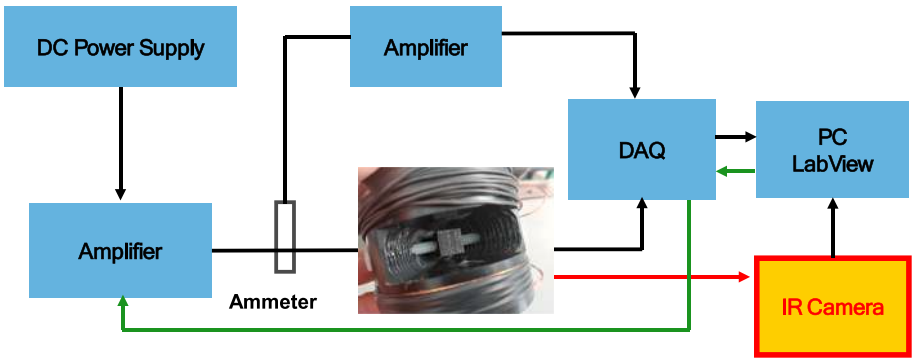

Fig. 9. Block scheme of proposed thermography analyses setup.

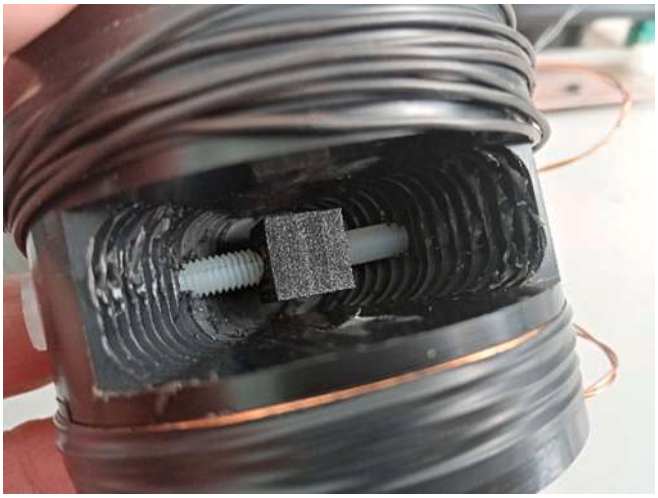

Fig. 10. Helmholtz coils as a thermal source.

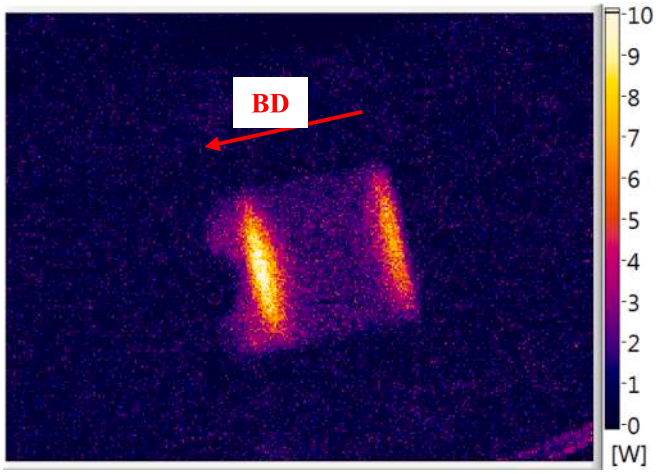

Fig. 11. Iron losses distribution with magnetization perpendicular to the growth direction.

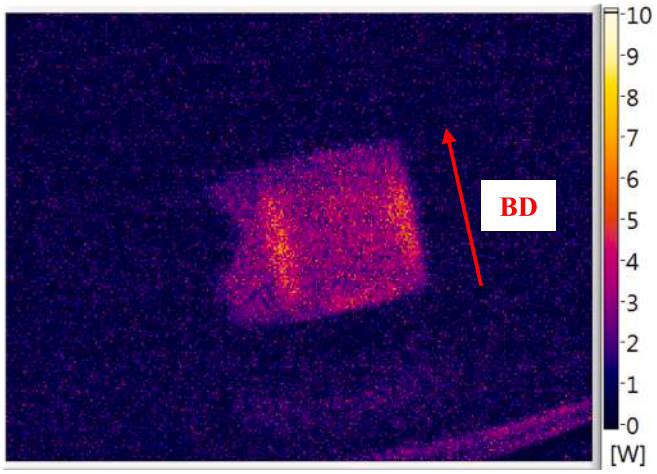

Fig. 12. Iron losses distribution with magnetization along the growth direction.

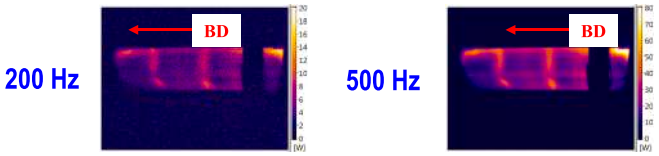

Fig. 13. Iron losses distribution with magnetization along the growth direction at different ranges of frequency for a bar sample.

use of an external excitation circuit. In this way, operating at different range frequencies and visualizing iron losses is possible, as shown in Fig. 13. Two iron losses distributions are considered at 200 Hz and 500 Hz. The average iron losses value for 200 Hz is about 5 W, and for 500 Hz, it is around 25 W. Also, it is possible to observe the local high losses, around 9 W for 200 Hz and 45 W for 500 Hz. These undesirable losses are probably due to defects during the process observed in some parts in Fig. 1. These defects are minor delaminations that cause high losses in AM components.

6. Conclusions

In conclusion, the use of additive manufacturing (AM) has revolutionized the manufacturing industry by enabling the production of complex geometries with high precision and accuracy. However, the AM process can lead to many defects and discontinuities that can compromise the performance and quality of the final product. Therefore, there is a need for effective methods to study and control losses in AM components. Active thermography is one such NDT technique that has shown great potential for the study of losses in AM components. The technique has several advantages, including being a non-contact and efficient method. It has been used to detect and characterize various defects in AM components.

In the case under exam, different defects have been observed both in metallographic analyses and via the thermographic method. Some results confirm the necessity for further optimization of the AM process for the proposed FeSi alloy. Moreover, the build direction and sample shape position play an important role in defining the iron losses. The designer has to pay attention to how to position pieces considering the final application, especially in the case of electromagnetic devices.

In the end, future activities consist of improving the IR camera resolution to observe the iron losses at the microscale and compare them to microstructure defects.

CRediT authorship contribution statement

Michele Quercio: Writing – review & editing, Writing – original draft, Methodology, Investigation, Formal analysis, Data curation, Conceptualization. **Emir Poskovic:** Writing – review & editing, Writing – original draft, Validation, Methodology, Data curation, Conceptualization. **Fausto Franchini:** Writing – review & editing, Writing – original draft, Validation, Methodology, Data curation, Conceptualization. **Elisa Fracchia:** Writing – review & editing, Writing – original draft, Methodology, Data curation, Conceptualization. **Luca Ferraris:** Writing – review & editing, Writing – original draft, Validation, Methodology, Data curation, Conceptualization. **Aldo Canova:** Writing – review & editing, Writing – original draft, Validation, Methodology, Data curation, Conceptualization. **Alberto Tenconi:** Writing – review & editing, Writing – original draft, Validation, Methodology, Data curation, Conceptualization. **Hans Tiismus:** Conceptualization, Resources. **Ants Kallaste:** Conceptualization, Resources.

Declaration of competing interest

The authors declare that they have no known competing financial interests or personal relationships that could have appeared to influence the work reported in this paper.

Data availability

No data was used for the research described in the article.

Acknowledgements

The part of research activities developed by Emir Pošković was carried out within the Ministerial Decree no. 1062/2021 and received funding from the FSE REACT-EU - PON Ricerca e Innovazione 2014-2020. This manuscript reflects only the authors' views and opinions, neither the European Union nor the European Commission can be considered responsible for them. This research work was funded by the Estonian Ministry of Education (**Grant PRG-1827**).

References

[1] J. Faludi, C.M. Van Sice, Y. Shi, J. Bower, O.M.K. Brooks, Novel materials can radically improve whole-system environmental impacts of additive manufacturing, ISSN 0959-6526, Journal of Cleaner Production 212 (2019) 1580–1590, https://doi.org/10.1016/j.jclepro.2018.12.017.

[2] A. Canova, G. Gruosso, M. Quercio, Characterization of electromagnetic device by means of spice models, International Journal of Emerging Technology and Advanced Engineering (2021), https://doi.org/10.46338/IJETAE0921_02.

[3] A. Kampker, P. Treichel, K. Kreisköther, R. Pandey, M. K. Büning and T. Backes, "Alternative Fabrication Strategies for the Production of Axial Flux Permanent Magnet Synchronous Motors for Enhanced Performance Characteristics," *2018 8th International Electric Drives Production Conference (EDPC)*, Schweinfurt, Germany, 2018, pp. 1-7, doi: 10.1109/EDPC.2018.8658341.

[4] R.P. Magisetty, N.S. Cheekuramelli, Additive manufacturing technology empowered complex electromechanical energy conversion devices and transformers, ISSN 2352-9407, Applied Materials Today 14 (2019) 35–50, https://doi.org/10.1016/j.apmt.2018.11.004.

[5] M. Quercio et al., "Characterization of LPBF produced Fe2.9wt.%Si for electromagnetic actuator," in IEEE Access, doi: 10.1109/ACCESS.2023.3337138.

[6] V. Chaudhary, S.A. Mantri, R.V. Ramanujan, R. Banerjee, Additive manufacturing of magnetic materials, ISSN 0079–6425, Progress in Materials Science 114 (2020) 100688, https://doi.org/10.1016/j.pmatsci.2020.100688.

[7] F. Bernier, M. Ibrahim, M. Mihai, Y. Thomas, J.-M. Lamarre, Additive manufacturing of soft and hard magnetic materials used in electrical machines, Metal Powder Report 75 (6) (2020) 334–343, https://doi.org/10.1016/j.mprp.2019.12.002.

[8] T.N. Lamichhane, L. Sethuraman, A. Dalagan, H. Wang, J. Keller, M. P. Paranthaman, Additive manufacturing of soft magnets for electrical machines—a review, ISSN 2542-5293, Materials Today Physics 15 (2020) 100255, https://doi.org/10.1016/j.mtphys.2020.100255.

[9] A. Selema, M. Beretta, M. Van Coppenolle, H. Tiismus, A. Kallaste, M.N. Ibrahim, M. Rombouts, J. Vleugels, L.A.I. Kestens, P. Sergeant, Evaluation of 3D-printed magnetic materials for additively-manufactured electrical machines, ISSN 0304-8853, Journal of Magnetism and Magnetic Materials 569 (2023) 170426, https://doi.org/10.1016/j.jmmm.2023.170426.

[10] H. Tiismus, A. Kallaste, A. Belahcen, T. Vaimann, A. Rassõlkin, D. Lukichev, Hysteresis measurements and numerical losses segregation of additively manufactured silicon steel for 3D printing electrical machines, Applied Sciences 10 (18) (2020) 6515, https://doi.org/10.3390/app10186515.
[11] H. Tiismus, A. Kallaste, T. Vaimann and A. Rassõlkin, "Eddy Current Loss Reduction Prospects in Laser Additively Manufactured Soft Magnetic Cores," *2022 International Conference on Electrical Machines (ICEM)*, Valencia, Spain, 2022, pp. 1511-1516, doi: 10.1109/ICEM51905.2022.9910679.
[12] V. Martin, F. Gillon, D. Najjar, A. Benabou, J.-F. Witz, M. Hecquet, P. Quaegebeur, M. Meersdam, D. Auzene, MIM-like additive manufacturing of Fe3%Si magnetic materials, ISSN 0304-8853, Journal of Magnetism and Magnetic Materials 564 (2) (2022) 170104, https://doi.org/10.1016/j.jmmm.2022.170104.
[13] C.V. Mikler, V. Chaudhary, T. Borkar, V. Soni, D. Choudhuri, R.V. Ramanujan, R. Banerjee, Laser additive processing of Ni-Fe-V and Ni-Fe-Mo permalloys: microstructure and magnetic properties, ISSN 0167-577X, Materials Letters 192 (2017) 9–11, https://doi.org/10.1016/j.matlet.2017.01.059.
[14] E. Pošković, F. Franchini, L. Ferraris, E. Fracchia, J. Bidulska, F. Carosio, R. Bidulsky, M. Actis Grande, Recent advances in multi-functional coatings for soft magnetic composites, MDPI Materials 14 (22) (2021).
[15] F. Nishanth, A.D. Goodall, I. Todd, E.L. Severson, Characterization of an axial flux machine with an additively manufactured stator, IEEE Trans. on Energy Conv. 38 (4) (Dec. 2023) 2717–2729, https://doi.org/10.1109/TEC.2023.3285539.
[16] L.M. Bollig, P.J. Hilpisch, G.S. Mowry, B.B. Nelson-Cheeseman, 3D printed magnetic polymer composite transformers, ISSN 0304-8853, Journal of Magnetism and Magnetic Materials 442 (2017) 97–101, https://doi.org/10.1016/j.jmmm.2017.06.070.
[17] S. -T. Wu, P. -W. Huang, T. -W. Chang, I. -H. Jiang and M. -C. Tsai, "Application of Magnetic Metal 3-D Printing on the Integration of Axial-Flow Impeller Fan Motor Design," *in IEEE Transactions on Magnetics*, **57**, no. 2, pp. 1-5, Feb. 2021, Art no. 8201205, doi: 10.1109/TMAG.2020.3014651.
[18] Z. -Y. Zhang, K. J. Jhong, C. -W. Cheng, P. -W. Huang, M. -C. Tsai and W. -H. Lee, "Metal 3D printing of synchronous reluctance motor," *2016 IEEE International Conference on Industrial Technology (ICIT)*, Taipei, Taiwan, 2016, pp. 1125-1128, doi: 10.1109/ICIT.2016.7474912.
[19] T. Q. Pham, T. T. Do, P. Kwon and S. N. Foster, "Additive Manufacturing of High Performance Ferromagnetic Materials," *2018 IEEE Energy Conversion Congress and Exposition (ECCE)*, Portland, OR, USA, 2018, pp. 4303-4308, doi: 10.1109/ECCE.2018.8558245.
[20] V. Popov, A. Koptyug, I. Radulov, F. Maccari, G. Muller, Prospects of additive manufacturing of rare-earth and non-rare-earth permanent magnets, ISSN 2351-9789, Procedia Manufacturing 21 (2018) 100–108, https://doi.org/10.1016/j.promfg.2018.02.199.
[21] E. Poskovic, L. Ferraris, F. Carosio, F. Franchini and N. Bianchi, "Overview on bonded magnets realization, characterization and adoption in prototypes," *IECON 2019 - 45th Annual Conference of the IEEE Industrial Electronics Society*, Lisbon, Portugal, 2019, pp. 1249-1254, doi: 10.1109/IECON.2019.8927827.
[22] L. Li, B. Post, V. Kunc, A.M. Elliott, M.P. Paranthaman, Additive manufacturing of near-net-shape bonded magnets: Prospects and challenges, ISSN 1359-6462, Scripta Materialia 135 (2017) 100–104, https://doi.org/10.1016/j.scriptamat.2016.12.035.
[23] R. Domingo-Roca, J.C. Jackson, J.F.C. Windmill, 3D-printing polymer-based permanent magnets, ISSN 0264-1275, Materials & Design 153 (2018) 120–128, https://doi.org/10.1016/j.matdes.2018.05.005.
[24] A. Shen, C.P. Bailey, A.W.K. Ma, S. Dardona, UV-assisted direct write of polymer-bonded magnets, ISSN 0304-8853, Journal of Magnetism and Magnetic Materials 462 (2018) 220–225, https://doi.org/10.1016/j.jmmm.2018.03.073.
[25] L. Li, K. Jones, B. Sales, J.L. Pries, I.C. Nlebedim, K. Jin, H. Bei, B.K. Post, M. S. Kesler, O. Rios, V. Kunc, R. Fredette, J. Ormerod, A. Williams, T.A. Lograsso, M. P. Paranthaman, Fabrication of highly dense isotropic Nd-Fe-B nylon bonded magnets via extrusion-based additive manufacturing, ISSN 2214-8604, Additive Manufacturing 21 (2018) 495–500, https://doi.org/10.1016/j.addma.2018.04.001.
[26] L. Li, A. Tirado, B.S. Conner, M. Chi, A.M. Elliott, O. Rios, H. Zhou, M. P. Paranthaman, A novel method combining additive manufacturing and alloy infiltration for NdFeB bonded magnet fabrication, ISSN 0304-8853, Journal of Magnetism and Magnetic Materials 438 (2017) 163–167, https://doi.org/10.1016/j.jmmm.2017.04.066.
[27] A. B. Baldissera, P. Pavez, P. A. P. Wendhausen, C. H. Ahrens and J. M. Mascheroni, "Additive Manufacturing of Bonded Nd–Fe–B—Effect of Process Parameters on Magnetic Properties," *in IEEE Transactions on Magnetics*, **53**, no. 11, pp. 1-4, Nov. 2017, Art no. 2101704, doi: 10.1109/TMAG.2017.2715722.
[28] I.S. Ramírez, F.P.G. Márquez, M. Papaelias, Review on additive manufacturing and non-destructive testing, ISSN 0278-6125, Journal of Manufacturing Systems 66 (2023) 260–286, https://doi.org/10.1016/j.jmsy.2022.12.005.
[29] R. Zimermann, E. Mohseni, E.A. Foster, M. Vasilev, C. Loukas, R.K.W. Vithanage, C. N. Macleod, D. Lines, M. Pimentel, E.E. Silva, S. Fitzpatrick, S. Halavage, S. McKegney, M. Khalid Rizwan, S. Gareth Pierce, S. Williams, J. Ding, In-process non-destructive evaluation of metal additive manufactured components at build using ultrasound and eddy-current approaches, ISSN 1526-6125, Journal of Manufacturing Processes 107 (2023) 549–558, https://doi.org/10.1016/j.jmapro.2023.10.063.
[30] S. Everton, M. Hirsch, P. Stravroulakis, R. Leach, A. Clare, Review of in-situ process monitoring and in-situ metrology for metal additive manufacturing, Mater. Des. 95 (2016), https://doi.org/10.1016/j.matdes.2016.01.099.
[31] Z. Snow, L. Scime, A. Ziabari, B. Fisher, V. Paquit, Scalable in situ non-destructive evaluation of additively manufactured components using process monitoring, sensor fusion, and machine learning, ISSN 2214-8604, Additive Manufacturing 78 (2023) 103817, https://doi.org/10.1016/j.addma.2023.103817.
[32] A. Lopez, R. Bacelar, I. Pires, T.G. Santos, J.P. Sousa, L. Quintino, Non-destructive testing application of radiography and ultrasound for wire and arc additive manufacturing, ISSN 2214-8604, Additive Manufacturing 21 (2018) 298–306, https://doi.org/10.1016/j.addma.2018.03.020.
[33] L. Ferraris, F. Franchini, E. Pošković, "A Novel Thermographic Method and Its Improvement to Evaluate Defects in Laminated and Soft Magnetic Composites Devices", *IEEE Trans. on Ind. Appl.*, **55** (6), pp. 5779-5788, Nov.-Dec. 2019, doi: 10.1109/TIA.2019.2933801.
[34] E. Pošković, L. Ferraris, G. Bramerdorfer, M. Cossale, A thermographic method to evaluate different processes and assembly effects on magnetic steels, IEEE Trans. Ind. Appl. 58 (3) (2022) 3405–3413.
[35] A. Palacios, L. Cong, M.E. Navarro, Y. Ding, C. Barreneche, Thermal conductivity measurement techniques for characterizing thermal energy storage materials – A review, ISSN 1364-0321, Renewable and Sustainable Energy Reviews 108 (2019) 32–52, https://doi.org/10.1016/j.rser.2019.03.020.
[36] M. Quercio, et al., Functional characterization of L-PBF produced FeSi2.9 Soft Magnetic Material, in: 2022 International Conference on Electrical Machines (ICEM), 2022, pp. 531–537, https://doi.org/10.1109/ICEM51905.2022.9910684.
[37] M. Quercio, et al., Electromagnetic shielding properties of LPBF produced Fe2. 9wt. % Si alloy, Journal of Physics Energy 5 (4) (2023) 045003, https://doi.org/10.1088/2515-7655/ace92f.
[38] M. Garibaldi, I. Ashcroft, M. Simonelli, R. Hague, Metallurgy of high-silicon steel parts produced using Selective Laser Melting, ISSN 1359-6454, Acta Materialia 110 (2016) 207–216, https://doi.org/10.1016/j.actamat.2016.03.037.
[39] M. Garibaldi, I. Ashcroft, N. Hillier, S.A.C. Harmon, R. Hague, "Relationship between laser energy input, microstructures and magnetic properties of selective laser melted Fe-6.9%wt Si soft magnets", *Materials Characterization*, doi: 10.1016/j.matchar.2018.01.016.
[40] G. Stornelli, B.R.R. Vargas, P. Folgarait, et al., Development of FeSi steel with increased Si content by laser powder bed fusion technology for ferromagnetic cores application: Microstructure and properties, MRS Adv. (2023), https://doi.org/10.1557/s43580-023-00646-7.
[41] T.F. Babuska, B.A. Krick, D.F. Susan, A.B. Kustas, Comparison of powder bed fusion and directed energy deposition for tailoring mechanical properties of traditionally brittle alloys, ISSN 2213-8463, Manufacturing Letters 28 (2021) 30–34, https://doi.org/10.1016/j.mfglet.2021.02.003.
[42] A. Di Schino, R. Montanari, M. Sgambetterra, G. Stornelli, A. Varone, G. Zucca, Heat treatment effect on microstructure evolution of two Si steels manufactured by laser powder bed fusion, ISSN 2238-7854, Journal of Materials Research and Technology 26 (2023) 8406–8424, https://doi.org/10.1016/j.jmrt.2023.09.155.
[43] D. Goll, D. Schuller, G. Martinek, T. Kunert, J. Schurr, C. Sinz, T. Schubert, T. Bernthaler, H. Riegel, G. Schneider, Additive manufacturing of soft magnetic materials and components, ISSN 2214-8604, Additive Manufacturing 27 (2019) 428–439, https://doi.org/10.1016/j.addma.2019.02.021.
[44] M. Garibaldi, I. Ashcroft, J.N. Lemke, M. Simonelli, R. Hague, Effect of annealing on the microstructure and magnetic properties of soft magnetic Fe-Si produced via laser additive manufacturing, ISSN 1359-6462, Scripta Materialia 142 (2018) 121–125, https://doi.org/10.1016/j.scriptamat.2017.08.042.
[45] E. Pošković, F. Franchini, L. Ferraris, F. Carosio, M. Actis Grande, Rapid Characterization Method for SMC Materials for a Preliminary Selection, MDPI Appl. Sci. 11 (24) (2021).
[46] C. Appino, E. Ferrara, F. Fiorillo, L. Rocchino, C. Ragusa, J. Sievert, T. Belgrand, C. Wang, P. Denke, S. Siebert, Y. Norgren, K. Gramm, S. Norman, R. Lyke, M. Albrecht, X. Zhou, W. Fan, X. Guo, M. Hall, International comparison on SST and Epstein measurements in grain-oriented Fe-Si sheet steel, Int. J. Appl. Electromagn. Mech. 48 (2015) 123–133.
[47] D. Miyagi, T. Yamazaki, D. Otome, M. Nakano, N. Takahashi, Development of measurement system of magnetic properties at high flux density using novel single-sheet tester, IEEE Trans. on Magn. 45 (10) (October 2009) 3889–3892.
[48] Z. Gmyrek, Single sheet tester with variable dimensions, IEEE Trans. Instrum. Meas. 65 (7) (2016) 1661–1668.
[49] E. Pošković, L. Ferraris, F. Franchini, R. Bidulsky, M. Actis Grande, "Novel SMC Materials with the Insulating Layer Treated at High Temperature", *EPMA EURO PM2019*, Maastricht (Netherlands), 13÷16 October 2019, Conf. Proc..